

Characterization of sizing layers and buried polymer/sizing/substrate interfacial regions using a localized fluorescent probe

Joseph L. Lenhart,^{a,*} Joy P. Dunkers,^a John H. van Zanten,^b and Richard S. Parnas^c

^a National Institute of Standards and Technology, Gaithersburg, MD 20899, USA

^b Chemical Engineering Department, North Carolina State University, Raleigh, NC, USA

^c Institute of Materials Science and Chemical Engineering Department, University of Connecticut, Storrs, CT, USA

Received 26 December 2001; accepted 17 September 2002

Abstract

A novel technique is described to investigate buried polymer/sizing/substrate interfacial regions, in situ, by localizing a fluorescent probe molecule in the sizing layer. Epoxy functional silane coupling agent multilayers were deposited on glass microscope cover slips and doped with small levels of a fluorescently labeled silane coupling agent (FLSCA). The emission of the grafted FLSCA was dependent on the silane layer thickness, showing blue-shifted emission with decreasing thickness. The fluorescent results suggest that thinner layers were more tightly bound to the glass surface. The layers were also characterized by scanning electron microscopy, contact angle, and thermogravimetric analysis (TGA). When the FLSCA-doped silane layers were immersed in epoxy resin, a blue shift in emission occurred during resin cure, indicating the potential to study interfacial chemistry, in situ. Thicker silane layers exhibited smaller fluorescence shifts during cure, suggesting incomplete resin penetration into the thickest silane layers.

© 2003 Elsevier Science (USA). All rights reserved.

Keywords: Fluorescence; Interface; Interphase; Composite; Epoxy; Coupling agent

1. Introduction

Polymer adhesion to a solid substrate is important in many technical applications including fiber and nano-reinforced composites, electronics, biomaterials, and adhesives [1]. Some of the many factors that influence the strength and durability of the polymer/substrate bond are the substrate roughness and surface energy, the viscoelastic properties of the polymer matrix and the buried interfacial region, the interaction between the substrate and polymer (i.e., van der Waals attractions and hydrogen or covalent bonding), the presence of a sizing layer on the substrate, the interpenetration, entanglement, and potential reactivity between the sizing and polymer, and processing issues (i.e., competition between polymerization kinetics and interfacial diffusion) [2,3].

Silane coupling agents are often applied to the substrate surface to promote polymer adhesion to the surface [4]. The

general formula for a silane coupling agent is $X_3Si(CH_2)_nY$, where X is a hydrolyzable group such as chlorine or an alkoxy, Y is the organic functional group chosen to provide compatibility with the resin, and “ n ” typically varies from 0 to 3. The coupling agent enhances adhesion because the hydrolyzed silicon end of the coupling agent can bond with the substrate surface (either hydrogen or covalent bonding), while the organic end is usually chosen to bind with the resin. This interfacial coupling is known to enhance the wet strength of fiber-reinforced composites [5] and decrease water adsorption at the substrate/polymer interface [6].

The structure of the silane layer depends on a number of factors including the layer thickness and amount of adsorbed material, the deposition procedure (i.e., solvent polarity, water content, pH, and substrate isoelectric point), the hydrolysis and condensation kinetics of the coupling agent, and the substrate/coupling agent interaction [7–11]. These factors will influence the amount, thickness, molecular orientation, bonding characteristics (chemisorbed or physisorbed), and morphology of the adsorbed coupling agent layer. Understanding the structure of the silane layers is important for interpreting their properties, and ability to

* Corresponding author. Current address: Sandia National Laboratory, Albuquerque, NM, USA.

E-mail address: jllenha@sandia.gov (J.L. Lenhart).

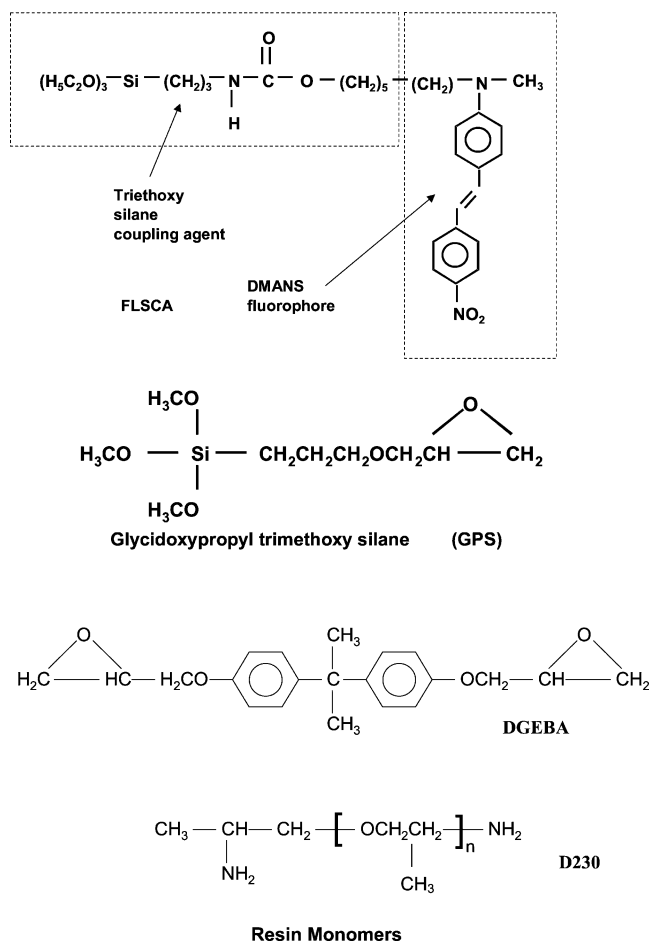


Fig. 1. The structure of the fluorescent labeled silane coupling agent, FLSCA (top), glycidoxypropyltriethoxysilane (GPS) (middle) and the resin monomers (diglycidyl ether of bisphenol A, DGEBA, and poly(propylene glycol) bis-2-aminopropyl ether, D230, bottom two).

influence the strength and durability of the polymer/substrate bond. For example, the amount of physically adsorbed silane material on silica was shown to impact the dynamic mechanical properties of silica-filled methacrylate composites [12]. The mobility of a silane layer was also shown to influence the flexural strength and fracture toughness of glass/epoxy composites [13].

In addition to the structure of the coupling agent layer, the interaction between the silane layer and the polymer resin is important (i.e., extent of interpenetration, strength of interaction, and extent of bonding or interaction) for determining the adhesive strength. For example, Wool and co-workers showed that the density of “sticker” groups in the polymer chains [14] and the density of reactive receptor groups in silane layers on a substrate [15] has a dramatic impact on the fracture toughness and adhesive strength of the polymer/substrate bond.

Owing to the complicated nature of adhesion and its dependence on processing, it would be beneficial to have an in situ probe capable of relating the buried interfacial structure to the adhesive properties. In this work, a silane coupling

agent molecule was tagged with a dimethylaminonitrostilbene fluorescent dye (DMANS), generating a fluorescently labeled silane coupling agent (FLSCA). The structure of FLSCA is shown in Fig. 1. Glycidoxypropyltriethoxysilane (GPS, see Fig. 1) coupling agent layers, on glass microscope cover slips, were doped with small levels of the FLSCA dye. In previous work we showed that FLSCA (grafted in silane layers) was sensitive to the surface energy of the coupling agent layers [16] and to the polymer dynamics in the buried interfacial region [17]. In this work we demonstrate that grafted FLSCA is sensitive to additional factors that influence adhesion, including (1) the structure of the silane layer on the surface and (2) interpenetration between the reacting resin and the silane layer.

It is important to understand that the silane layer we use in this work is only a model for a primer coating that is used to promote adhesion in industrial applications. For example, in glass fiber reinforced composites the sizing package/primer is composed of a film former, lubricant, and antistatic agent in addition to the silane coupling agent [18]. Also, industrial sizing coatings can be applied by many different techniques, including absorption, dip or spin casting, spraying, and even rolling or brushing techniques similar to painting a wall. The fluorescent technique we describe in this paper is generally applicable to different sizing/primer types and application methods. We demonstrate in this work that the fluorescent dye is sensitive to the structure of a model sizing layer and interpenetration between the sizing and a curing resin, illustrating a generalized technique to study buried substrate/sizing/polymer interfacial regions by localizing a fluorescent probe into the sizing layer.

2. Experimental

The uncertainty given in the experimental procedure description, or shown in the experimental results, represents a range of values. For some of the experimental results, the uncertainty is shown as a standard deviation based on measurements taken on at least four samples and multiple measurements per sample. When a standard deviation is used, the symbol (sd) will appear after the number as an indication.

Unless otherwise stated, all chemicals were used as obtained from Aldrich Chemical Company (Milwaukee, WI) [19]. FLSCA was synthesized by a method described previously [16,20–22]. FLSCA was diluted in the deposition solution with glycidoxypropyltrimethoxysilane (GPS). GPS was used as received from Gelest (Tulleytown, PA).

Coupling agent layers were grafted to glass microscope cover slips (Fisher Scientific, Pittsburgh, PA) using an ethanol-based deposition procedure as described previously [16,23]. GPS and FLSCA were added to an ethanol/water mixture with the volume fraction of ethanol equal to 95%, under slightly acidic conditions. To adjust the thickness of the silane layers, the total silane concentration in the

ethanol/water mixture was varied from 0 to 0.2 mmol/ml (0 to 5 v/v %). The molar ratio of FLSCA to GPS in the deposition solution ranged from 0.004 to 0.006. After hydrolysis of the coupling agents, clean glass microscope cover slips were dipped into the deposition solution. The glass surface was exposed to the coupling agent solution for (10 ± 1) min. The cover slips were then rapidly removed from the solution with tweezers and leaned against a glass beaker at an $80^\circ \pm 5^\circ$ angle relative to the horizontal. While solution was initially entrained on the cover slips, the solution rapidly flowed down to the bottom of the cover slip and was absorbed by a paper cloth. The cover slips were left in a vertical position to air dry for (5 ± 1) min. The coated cover slips were then cured at $(100 \pm 2)^\circ\text{C}$ for (1.5 ± 0.2) h. After this cure, the cover slips were washed by two successive dips in clean ethanol for 30 ± 5 s. During the ethanol dip, the coated cover slips were vigorously shaken. The purpose of this wash was to remove excess dye and weakly adsorbed coupling agent that had deposited on the surface during solvent evaporation. The washed cover slips were dried for (1 ± 0.1) h at $(100 \pm 2)^\circ\text{C}$. After drying, the samples were sealed in glass vials and stored in the dark until fluorescence measurements were made the following day. Measurements were made near the center of the coated cover slips.

This deposition procedure was chosen for simplicity. We chose a silane deposition procedure where structural changes in the silane coating could be induced by small changes in the procedure. Again, the objective is to illustrate that a localized fluorescent dye is sensitive to these structural changes and thus offers potential for in situ monitoring of buried interfacial properties. Other deposition procedures are also viable options as this localized fluorescence technique can be generalized for studying different primer/sizing types and application methods. The thickness and structure of the silane coupling agent coating can depend on many factors, including the silane concentration in solution, the solution viscosity, the solvent evaporation rate, and the substrate withdrawal speed from the deposition solution [24]. However, a plot of the silane layer thickness and fluorescence intensity showed a linear relationship with the silane concentration in the deposition solution, illustrating that we were able to effectively control the layer thickness by adjusting the solution concentration. This was not unexpected as other coating techniques, such as spin casting for example, generally give thicker coating layers with increasing solution concentrations.

While only the thickness of the ethanol-washed silane coupling agent layers was measured, fluorescence measurements were made on some of the samples before and after the ethanol wash. These samples exhibited a $(50 \pm 10)\%$ decrease in the fluorescence intensity due to the two successive ethanol immersions after cure. It is generally accepted that silane coupling agents exhibit multilayer structures [4, 10, 25]. For example, it has been proposed that three layers are present. The outer layer is physically adsorbed and com-

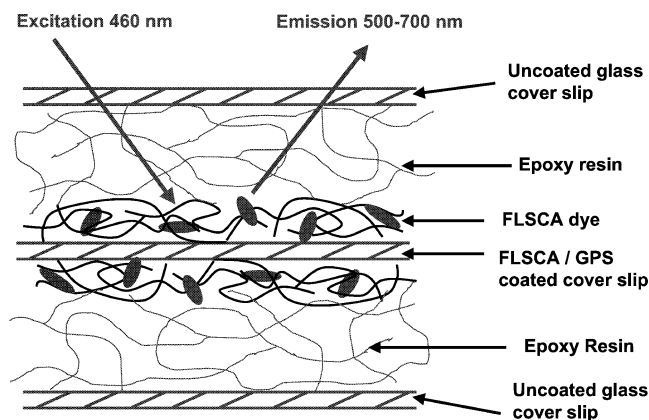


Fig. 2. The FLSCA/GPS layers were sandwiched with a thick layer of epoxy resin between two uncoated glass microscope cover slips. The fluorescent emission of grafted FLSCA was measured before and after the epoxy cured.

prises the majority of the coating. This outer layer can be hundreds of monolayer equivalents thick. The weakly bound outer layer is easily removed by a gentle solvent or water rinse. The second layer is more tightly bound, but can be removed by more aggressive treatments such as several hours of submersion in boiling water. The monolayer closest to the substrate is strongly chemisorbed and is very difficult to remove [25]. We observed a similar structure with the silane layers used in this study. A large fraction of the layer could be removed by the ethanol wash. A second fraction could be removed by immersion in boiling water. A small fraction was left on the glass substrates and was detectable by contact angle measurements.

The glass microscope cover slips were cleaned by immersion for (0.5 ± 0.05) h in NoChromix/sulfuric acid cleaning solution. The cover slips were then rinsed thoroughly with water, followed by a rinse in spectral-grade acetone. The clean cover slips were dried in an oven at 100°C prior to use.

After the FLSCA/GPS layers were grafted to the glass cover slips, each coated cover slip was sandwiched with uncured epoxy resin between two uncoated glass cover slips as is shown by Fig. 2. The range of the thickness of the epoxy resin in the sandwich was $(25 \text{ to } 100) \mu\text{m}$. Excitation light was sent through the uncoated cover slip and the epoxy resin. The fluorescence was collected from the FLSCA/GPS layer for both uncured resin and cured resin. The samples were cured for (4 ± 0.1) h at $(100 \pm 2)^\circ\text{C}$, followed by a (1 ± 0.1) h postcure at $(130 \pm 5)^\circ\text{C}$. For samples of DMANS or FLSCA in bulk epoxy, the center cover slip in the sample sandwich was not coated with a FLSCA/GPS coupling agent layer, but the dye was dissolved into the bulk epoxy resin used in the sample sandwich.

The resin system used in this study was an amine-hardened epoxy system. It was composed of a stoichiometric mixture of diglycidyl ether of bisphenol A (Tactix 123, Dow Chemical Company) and poly(propylene glycol) bis(2-amino propyl ether), (Jeffamine D230, Aldrich Chemical Company). For the amine hardener, the number average

molecular mass was 230 g/mol. The structure of these monomers is shown in Fig. 1. The two components were mixed together with a mechanical stirrer and then degassed under vacuum for (10 ± 1) min prior to use. At room temperature, this resin system reacts slowly, so a negligible amount of reaction occurs during mixing and degassing. Neither the Tactix resin nor hardeners were further purified.

Scanning electron microscopy (SEM) was used to measure the thickness of the silane coupling agent layers. After the coupling agents were deposited onto the glass microscope cover slips, the glass surface was scored with a diamond tip razor. The sample was snapped and mounted vertically onto the SEM mount. Carbon paint was used to mount the glass sample. After the carbon paint dried, the sample was coated with gold. SEM measurements were made on the unscored side of the cross-sectioned sample with a Hitachi S4500 field emission SEM using a working distance of 7 mm and an accelerating voltage of 7 kV. The upper secondary (in-lens) detector was used.

Contact angle measurements in water were made on the samples using a CAHN DCA 322 dynamic contact angle analyzer (Madison, WI). The contact angle was measured for four successive cycles. Contact angle values of the final cycle are reported here. Each measurement cycle involved the following steps: (1) tare the balance, (2) detect the sample contact with water, (3) advance the sample into the water a length of 4 mm, (4) hold the sample in this position for 2 min, and (5) recede the sample out of the water and return the motor to the starting position. The advancing and receding speed was 80 $\mu\text{m/s}$.

Fluorescence data were measured using a Spex Fluorolog Fluorimeter (Edison, NJ) in the right angle geometry collection mode. To minimize the signal due to reflected excitation light, samples were placed at a 60° angle relative to the incidence light. The excitation and emission slit widths were 2.5 mm. All emission spectra were measured at room temperature, $(25 \pm 1)^\circ\text{C}$, to eliminate temperature-dependent fluorescence effects.

UV/vis absorption measurements were made using a Perkin-Elmer Lambda 9 UV-vis-NIR spectrophotometer (Norwalk, CT). A deuterium lamp was the UV source and a tungsten-halogen lamp was the visible source. The detector was a photomultiplier tube. A bandpass of 1 nm and a scan rate of 240 nm/min were used to make the absorption measurements.

3. Results and discussion

Figure 3 shows typical absorption and emission spectra from a FLSCA/GPS layer grafted to a glass cover slip. In Fig. 3, the layers were not immersed in epoxy resin. The curves were normalized with the intensity at the respective absorption or emission maximum. The absorption maximum occurs at $(455 \pm 5 \text{ sd}) \text{ nm}$. The emission maximum for this layer occurs at $(640 \pm 2 \text{ sd}) \text{ nm}$. Little overlap occurs be-

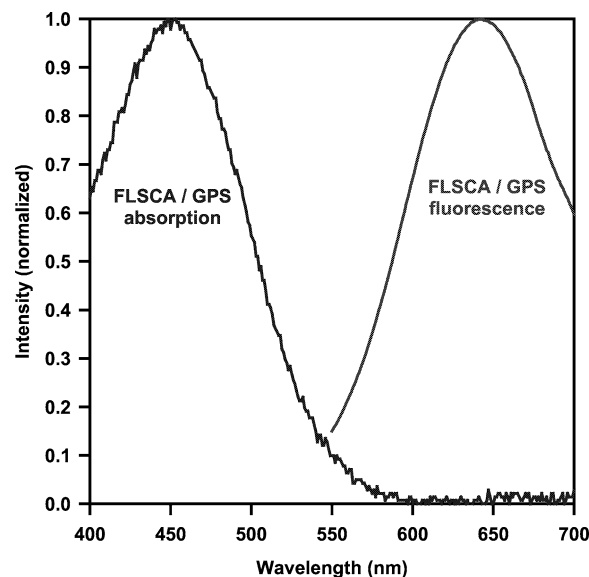


Fig. 3. Typical absorbance and emission spectra of a FLSCA/GPS layer prior to immersion in epoxy resin.

tween the absorption and emission spectra. In addition, the absorption is very small in the region of the fluorescence emission. This is important and demonstrates that inner filter effects do not skew the fluorescence emission or distort the position of the emission maximum. The absorption of the epoxy resin was also small in the regions of the fluorescence emission.

Figure 4 shows typical SEM scans of a thick and thin coupling agent layer as deposited on the glass cover slips. Both scans were taken at a magnification of 70,000. The glass can be seen at the left of both scans. The central band is the silane coupling agent layer. The dark region to the right is simply the vacuum in the SEM chamber. When the glass surface was cross-sectioned, fracture lines formed perpendicular to the surface. The fracture lines are illustrated in Fig. 4 with arrows. It is apparent that the fracture lines did not penetrate into the coupling agent coating. This was one way to verify that the band in the center was actually a surface coating, rather than simply a change in the glass topography. An uncoated cover slip utilized as a control exhibited the fracture lines but no thin band near the surface.

The coupling agent layer thickness was found to depend on the coupling agent concentration in the deposition solution. The thickness data are tabulated in Table 1. SEM results are reported for just the three thickest layers because the technique was not capable of resolving silane layers thinner than $\approx 50 \text{ nm}$. The SEM results illustrate several interesting observations. First, the coupling agent coatings were highly nonuniform (on a single sample and between different samples prepared by the same procedure), as indicated by the large standard deviations for the layer thickness. Second, the surface coverage appeared less complete for thinner layers. For the case of the two thickest layers, i.e., those obtained at $(0.1 \text{ and } 0.2) \text{ mmol/ml}$, SEM performed at various positions indicated that the film completely coated the glass surface.

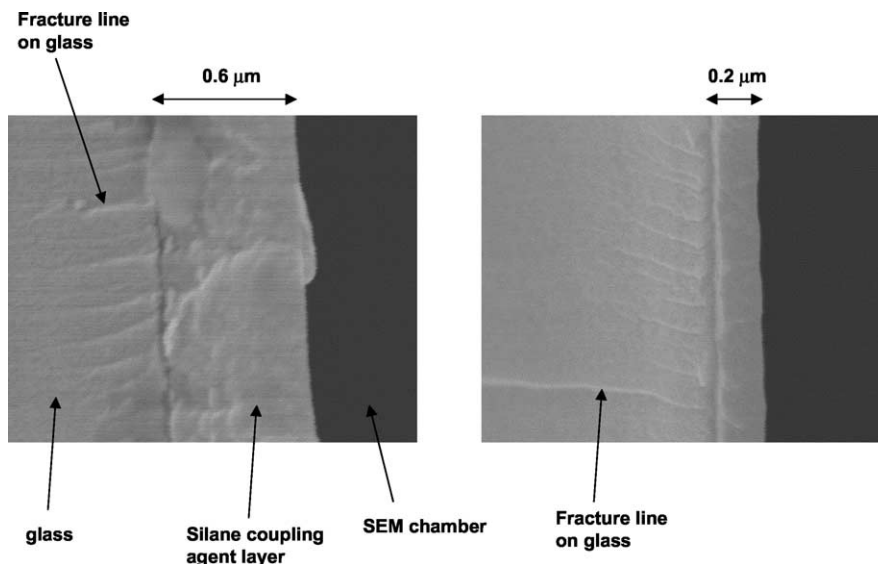


Fig. 4. SEM images of the FLSCA/GPS coatings on the glass surface.

Table 1

Contact angle (deg) and silane layer thickness (μm) as a function of the deposition concentration; Uncertainty is given as a standard deviation from measurements made on at least four samples

Solution concentration (mmol/ml)	Contact angle		Thickness (μm)
	Advancing	Receding	
0.2	70 ± 2	40 ± 2	0.52 ± 0.25
0.1	66 ± 2	42 ± 2	0.30 ± 0.15
0.05	65 ± 3	41 ± 2	0.18 ± 0.10
0.038	64 ± 2	42 ± 2	
0.025	64 ± 2	37 ± 2	
0	36 ± 3	8 ± 2	

However, a thinner film 0.05 mmol/ml contained regions where SEM detected no coupling agent and regions where SEM detected an “island” of coating. For layers deposited with silane concentrations less than 0.05 mmol/ml, the cover slip was primarily composed of regions where SEM could not detect any layer. From the SEM data, it was unclear whether these regions were a bare glass surface or very thin regions of coating (possibly only a few monolayers thick). The uncertainty in the thickness measurement is defined here as a standard deviation from measurements of four samples using 10 measurements per sample at random positions.

To further assess the coupling agent surface coverage, contact angle measurements were conducted on the various samples. The results are also reported in Table 1. The advancing and receding contact angles of the coated cover slips were much larger than the uncoated control, thereby verifying the presence of a silane coupling agent on the surface even when the most dilute deposition concentrations were used.

Figure 5 shows the variation of the wavelength of the fluorescence intensity maximum from the FLSCA/GPS layer with the total silane concentration in the deposition solution (thickness). As the layer thickness decreased, the emis-

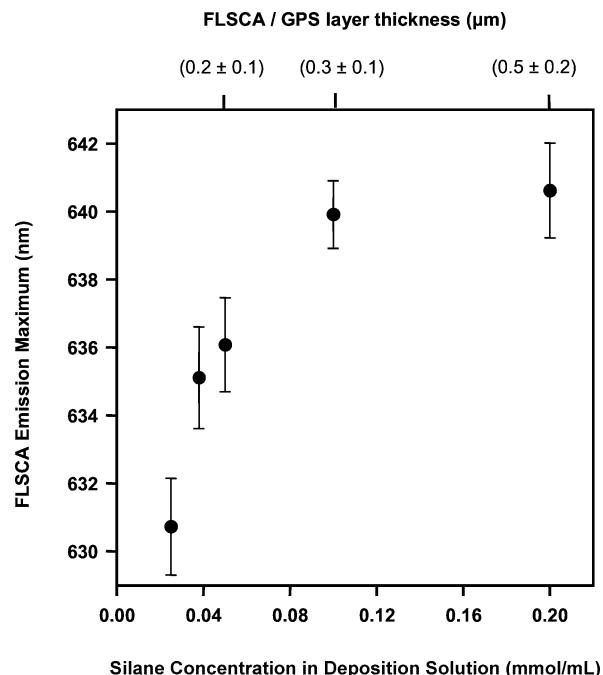


Fig. 5. The fluorescence emission maximum from FLSCA/GPS layers as a function of the silane concentration in the deposition solution (layer thickness).

sion maximum occurred at shorter wavelengths (blue-shifted emission). The emission maximum was essentially the same for the two thickest layers corresponding to 0.1 and 0.2 mmol/ml. This is not surprising as SEM of these thickest layers indicated significant overlap in the layer thickness (Table 1). As the layers become thinner, the fluorescence maximum is blue-shifted (i.e., to shorter wavelengths). Since the FLSCA emission is sensitive to its surrounding environment, the blue-shifted fluorescence emission suggests that thinner layers have a different structure than the thicker layers.

The Lippert equation describes how the solvent environment surrounding a dye molecule can influence the position of its fluorescence emission [26],

$$\nu_a - \nu_f \cong \frac{2}{hc} \left(\frac{\varepsilon - 1}{2\varepsilon + 1} - \frac{n^2 - 1}{2n^2 + 1} \right) \frac{(\Delta\mu)^2}{a^3} + \text{const}, \quad (1)$$

where ε is the solvent dielectric constant, n is the refractive index of the solvent, c is the speed of light, h is Planck's constant, a^3 is the volume occupied by the fluorophore, $\Delta\mu$ is the dipole moment difference of the fluorophore between the ground and excited states, and ν_a and ν_f are the wavenumbers (cm^{-1}) of the absorption and emission intensity maximum, respectively.

The Stokes shift is defined as the difference between the absorption and emission intensity maximum of the fluorophore. It is a measure of the energy dissipated from the excited state molecule before releasing a fluorescence emission. The refractive index contribution accounts for the ability of the solvent electrons to reorient to stabilize the dipole moment of the fluorophore. The dielectric constant term accounts for the solvent relaxation process, which decreases the energy difference between the ground and excited states. The constant term in Eq. (1) accounts for additional mechanisms of energy dissipation, such as vibrational relaxation.

In Eq. (1) the important terms involving the silane coupling agent environment (surrounding grafted FLSCA) are the dielectric constant and refractive index terms. If the local dielectric constant decreases, the Stokes shift is smaller, resulting in blue-shifted emission. A change in the dielectric constant that is observed by the excited dye can be caused by three factors: (a) a change in the dielectric relaxation time, (b) a change in the dipole strength of the molecules (polarity), and (c) a change in molecular orientation which can alter the local environment. The refractive index can also change if the silane layer density changes. These factors are discussed in detail below.

First, the dielectric relaxation time of the coupling agent layer can change with the layer thickness. In general, the dye is expected to be sensitive to changes in dielectric mobility of the surrounding medium if the distribution of dielectric relaxation times overlaps with the fluorescent lifetime of the excited dye. The fluorescent lifetime of DMANS is ~ 5 ns. Measurements of aminopropyltriethoxysilane (APS) layers on glass surfaces indicate that the dielectric relaxation of APS ranged from 4 to 10 ns [27]. Therefore, it is quite possible that GPS coupling agent layers could also exhibit dielectric relaxation times on the order of the FLSCA fluorescence lifetime. The blue-shifted emission from ever thinner GPS coupling agent layers suggests that the dielectric relaxation time of the silane coupling agent layer increases with decreasing layer thickness. This conclusion is not unreasonable. Decreasing mobility with decreasing layer thickness has also been observed by nuclear magnetic resonance spectroscopy (NMR) measurements of amino-functional silane layers grafted onto silica particles [28].

If the dipole moments of the molecules surrounding the FLSCA probe decreased (less polar environment), then a blue shift in emission would be observed (see Eq. (1)). The silane coupling agent layer contact angles remain essentially constant, thereby indicating that the dipole moment on the surface of the FLSCA/GPS layer did not significantly change with layer thickness. Contact angle is only sensitive to the surface polarity of the silane layer and cannot detect changes in the dipole moments in the bulk of the layer. However, if a change in the bulk polarity of the layer did occur, then this could manifest itself by a change in the surface polarity and a change in contact angle.

The silane molecule orientation near the FLSCA probe molecules could alter the local dielectric constant observed by the excited dye. ^{29}Si -NMR measurements of methacryloxypropyltrimethoxysilane (MPS) layers on colloidal silica indicated that the coupling agent adsorption behavior was dependent on the coupling agent concentration in the deposition solution [29]. For low MPS concentrations, coupling agent dimers adsorbed to the surface in an ordered fashion. At higher MPS concentrations, coupling agents were randomly adsorbed. The fluorescence measurements described here cannot delineate whether the blue shift (from thinner GPS layers) is caused by slower dielectric relaxation or increased orientation. Fluorescence anisotropy could provide insight about the dye orientation on the surface but has not been conducted. This is a focus of ongoing work.

In addition to changes in the local dielectric environment of the FLSCA/GPS layer, refractive index changes with layer thickness can lead to the blue shift in emission (Fig. 5). The silane layer refractive index is directly proportional to the density of polarizable groups in the layer. The increase of density may increase the refractive index, which in turn will lead to a smaller Stokes shift (Eq. (1)) and blue-shifted emission [26]. The shorter wavelength emission (blue-shifted) observed with decreasing coupling agent layer thickness (Fig. 5) could be a result of increasing density. The density increase could be caused by increased silane molecule orientation or packing efficiency near the glass surface.

It is possible that the emission will be sensitive to stress since this can potentially change the local dielectric constant by inducing film orientation. Croll showed that polymer films cast from toluene had residual stress due to solvent evaporation and that the stress was independent of the film thickness and initial solution concentration [30]. However, since silane layers are known to exhibit nonhomogeneous structure through the layer thickness, it is likely that the stress during silane cure will be dependent on film thickness. In particular, stress development during the ethanol evaporation would be caused if the resulting film shrinkage were restricted in the plane of the substrate. This is likely true for the strongly chemisorbed portion of the layers closest to the glass surface. However, it is possible that physically adsorbed portions of the layer are not constrained lateral to the substrate, leading to a nonuniform stress in the silane film.

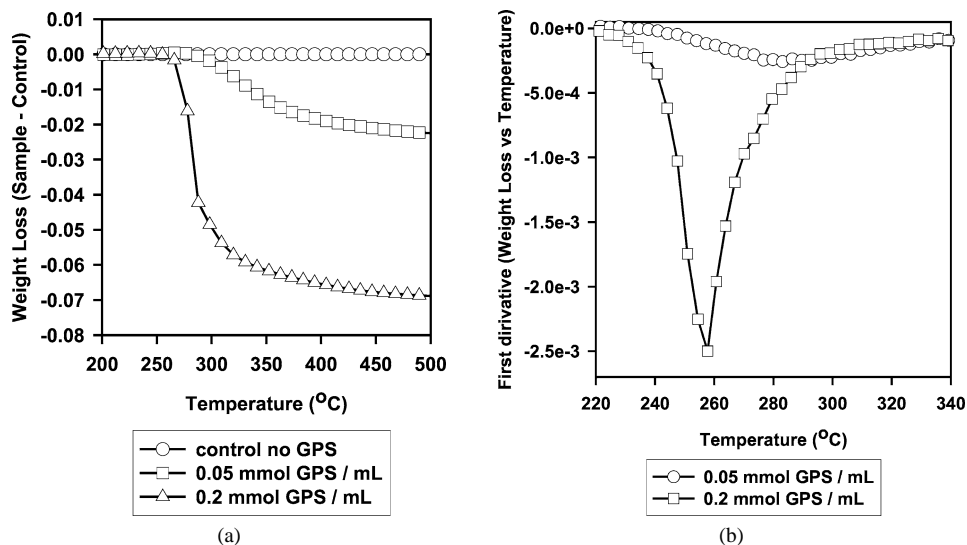


Fig. 6. (a) The fractional mass loss as a function of temperature is shown for two GPS coatings on silica powder. The GPS coatings were deposited by immersing the silica powder in two different deposition solution concentrations. The mass loss of a control, which contained no GPS in the deposition solution, was subtracted from the data. (b) The first derivative of the mass loss versus temperature is shown. The maximum of the derivative occurs at higher temperatures for the GPS coating deposited from the lower silane concentration deposition solution.

A variation in the film stress with thickness can potentially explain the changes in the emission maximum. Currently, the sensitivity of the fluorescent probe to stress has not been adequately studied. We have started experiments in this area by dissolving the dye in bulk polymer networks and monitoring the emission under load.

It is clear that the FLSCA fluorescence emission indicates changes in the coupling agent structure with decreasing silane layer thickness. While it is difficult to ascertain the exact cause of the blue shift with decreasing silane layer thickness, possible explanations include hindered layer mobility, increased orientation, increased silane layer density, or increased stress in thinner films. All of these factors have been observed to occur in silane layers by alternative techniques. These phenomena are associated with more tightly bound coupling agent molecules.

Thermogravimetric analysis (TGA) was utilized to probe the strength of the silane coupling agent layer binding. A thick and thin GPS layer (without the FLSCA dye) was grafted onto high surface area silica powder ($300 \text{ m}^2/\text{g}$ from Gelest, Tullytown, PA) using a similar deposition procedure. The silica powder was cleaned by vigorous shaking in spectral-grade acetone for 30 min. The powder was dried under vacuum overnight at 100°C . After cleaning and drying, the powder was immersed in a hydrolyzed GPS solution (similar to the description in the Experimental section). After absorption of the silane coupling agents, the powder was filtered in a centrifuge and separated from the ethanol solution. The coated powder was then dried under vacuum and cured similar to the glass slides. After curing, the powder was washed vigorously in clean ethanol, filtered in a centrifuge and separated from the solution, and dried under vacuum again. The TGA measurements were conducted by initially holding the sample at 150°C for

30 min to remove any residual water or ethanol due to the deposition procedure. Once the mass loss was negligible at 150°C , the sample was ramped to 800°C at $5^\circ\text{C}/\text{min}$. The TGA mass loss was independent of the temperature ramp rate for rates below $10^\circ\text{C}/\text{min}$. Figure 6 shows TGA data for the two GPS coatings of different thickness on silica powder. Figure 6a shows the mass loss fraction as a function of temperature for the layers. A control sample was measured for silica powder immersed in the ethanol deposition solution that contained no silane coupling agent. The control sample showed a small mass loss, probably due to residual impurities adsorbed to the powder. The data in Fig. 6a actually show the mass loss fraction for the samples after the mass loss from the control sample was subtracted. The data clearly illustrates that, for higher GPS solution concentrations, more material is present on the powder. Figure 6b plots the slope of the TGA mass loss as a function of temperature. The maximum negative slope indicates a point where the layer is removed most rapidly with increasing temperature. The GPS layer deposited from a lower concentration silane solution (GPS concentration = $0.05 \text{ mmol}/\text{ml}$ in the deposition solution) was removed at temperatures ranging from (20 to 30) $^\circ\text{C}$ higher than the layer deposited from the higher concentration solution.

Certainly it is difficult to make a direct comparison between the structure of the silane layers on the glass microscope cover slips and on the silica powder. For example, due to the different cleaning and deposition procedure used to coat the silica powder, and possible surface chemical differences between the glass cover slips and the silica powder, the silane layers on the two surfaces could have different structures. In addition, the silica powder is porous, which can potentially influence the coupling agent surface bonding. The TGA data, however, was not influenced by diffusion

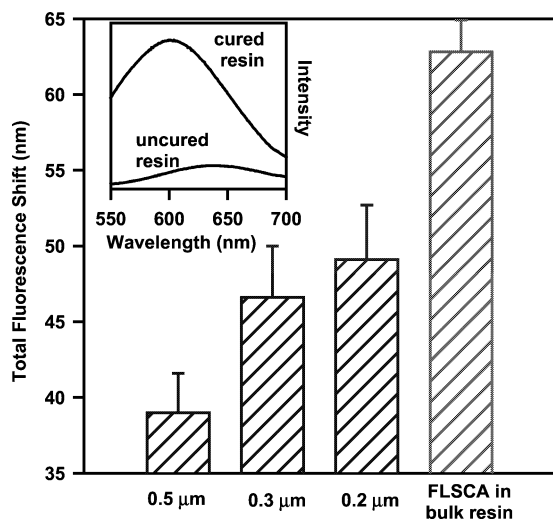


Fig. 7. The inset shows a typical fluorescence emission spectra for a FLSCA/GPS layer immersed in the epoxy sandwich, both before and after resin cure. The total fluorescence maximum shift during resin cure depends on the FLSCA/GPS layer thickness, with thinner layers exhibiting smaller shifts. The error bars represent a standard deviation from multiple measurements made on at least six samples. The standard deviation of the layer thickness was 50% of the value given.

of the silane layer out of the porous structure, as the mass loss data was independent of the heating rate for rates below 10 °C/min. In addition, at the silane deposition concentrations used in TGA study, it is likely that significant polymerization of the silane molecules occurs in the solution prior to adsorption. Therefore, it is possible that the silica pores were actually blocked rather than completely filled. Despite these potential criticisms of the TGA experiments, the mass loss versus temperature curves present qualitative evidence, suggesting that thinner silane layers are more tightly bound to the substrate, further supporting our interpretation of the fluorescence data.

Although the initial structure of the silane coupling agent layer can influence the strength and durability of the adhesive bond, the interaction between the silane layer and the resin is equally important. To probe the sensitivity of grafted FLSCA to the coupling agent/resin interaction, FLSCA/GPS layers of varying thickness were immersed in epoxy resin. The emission spectrum of FLSCA was measured before and after resin cure. The inset in Fig. 7 shows typical fluorescence emission from the FLSCA/GPS layer before and after epoxy cure. Both a blue shift in the emission maximum and an increase in the fluorescence intensity occurred during cure. This change in the fluorescence emission gives the technique potential for studying the interfacial cure reaction.

The intensity increases most likely due to two factors: (1) a decreased dielectric constant observed by the excited dye and (2) decreased free volume following resin cure [16,17,23,31]. For DMANS and FLSCA dyes, nonradiative energy dissipation mechanisms involve excited state isomerization reactions such as trans to cis isomerization (TCI) or twisted internal charge transfer (TICT). Owing to these different

isomerization mechanisms, DMANS has its highest quantum yield in solvents of intermediate polarity [32,33]. The TICT states are stabilized in polar environments (i.e., uncured epoxy resin), resulting in low fluorescence intensity with these solvents. When the dielectric constant of the resin decreases during cure, the TICT states become less stable and an increase in intensity is observed. In very low dielectric environments the TCI state is favored. Since the cis isomer of DMANS is not fluorescent, the intensity will decrease. With the epoxy resin, we have not observed decreases in intensity at high extents of cure, suggesting that the TICT state is the dominant nonradiative mechanism in the epoxy resin environment. As the resin cures, the TICT state is less favored and the intensity increases. A decrease in resin free volume during cure will also cause the intensity increase. Both TCI and TICT isomerizations require rotation of the dye molecule. As the resin free volume decreases, the dye rotation is restricted, slowing the kinetics of these nonradiative pathways and resulting in higher intensity.

The emission blue shift during resin cure is due to the decreasing dielectric constant that is observed by the dye, and the increase in the resin refractive index during cure as was discussed previously. This shift is predicted by Eq. (1) and is discussed in detail in previous publications [16,17,23]. Because no internal standard is present in the emission spectra, it is more practical to monitor the wavelength shift during cure. The inset in Fig. 7 shows that the emission spectra have a high signal-to-noise ratio and the emission maximum can be measured to ± 1 nm. Figure 7 also illustrates the total fluorescence shift during resin cure for FLSCA/GPS layers of varying thickness. The total shift for FLSCA dissolved in bulk epoxy is also shown. First, it should be noted that the shift for the dye in bulk resin was much larger than the shift from any of the FLSCA/GPS layers. This indicates that the interfacial structure is different from the bulk resin. An earlier report demonstrated that the dye emission maximum was not distorted due to dye concentration, covalent bonding with the silane layer, or tethering of the dye to the silane coupling agent tail [23]. In the absence of these artifacts, changes in the fluorescence shift suggest differences in the interfacial chemical composition.

The fluorescence maximum shift from grafted FLSCA/GPS layers during resin cure suggests that the resin monomers are able to penetrate and possibly react with the coupling agent layer. It is well-established that fluorescence shifts from a dye can be related to the extent of a resin cure reaction [31,34–36]. Since the GPS molecule contains an epoxy functional group, it is known that GPS can participate in the cross-linking reaction with the amine groups on the D230 hardener. The blue shift in fluorescence from FLSCA demonstrates that resin monomers are able to penetrate into the silane layer. If no resin penetrated the silane layer, then the local environment surrounding FLSCA would not change and no shift would be observed. The emission from FLSCA in bulk DGEBA or in bulk D230 is near 628 and 639 nm, respectively. In a stoichiometric mixture of the

two monomers, the FLSCA emission maximum occurs near 630 nm. Since the emission maximum for FLSCA/GPS layers ranged between 630 and 642 nm, it is unlikely that the diffusion itself of the resin monomers into the silane layer would cause the fluorescence shift. The fluorescence shift must be due to a chemical reaction between the hardener and the GPS molecules, or between DGEBA and D230 monomers that have diffused into the silane layer. The smaller shift from thick layers suggests that the resin does not completely penetrate or react with these layers. The incomplete penetration is likely caused by a competition between monomer diffusion into the layer, and the resin reaction, which slows the diffusion process. For thick layers the resin may gel before complete interpenetration.

The fluorescence maximum shift from the two thinnest silane layers (i.e., those from 0.038 and 0.025 mmol/ml silane concentration in the deposition solution) was not determined following immersion in epoxy because the fluorescence signal from these layers was too low. As the epoxy resin is intrinsically fluorescent, when the thinnest layers were immersed in the resin, the background fluorescence signal from the epoxy resin was of the same order of magnitude as the fluorescence signal from the FLSCA/GPS layer. It was therefore difficult to subtract this background signal and extract the true FLSCA/GPS fluorescence response. For the thicker layers, the background signal from the epoxy resin was small compared to the emission spectrum of the silane layer. Dyes with higher quantum yields than the DMANS fluorophore used in this study are currently under investigation. Literature values suggest that the DMANS quantum yield in polar environments, like an epoxy resin, is < 0.01 [32,33]. A dye with a quantum yield close to unity would increase the fluorescence signal by orders of magnitude and therefore much thinner silane layers could be successfully utilized. Of course, the dye attachment chemistry will need to be developed. However, other photoactive groups (besides DMANS) have recently been attached to silane coupling agent tails [27,37,38], so the chemistry may already be available in the literature.

4. Conclusions

This manuscript describes a novel technique to study buried polymer/sizing/substrate interfacial regions, in situ, by localizing a fluorescent probe molecule in the sizing layer. In particular, glycidoxypolytriethoxysilane coupling agent (GPS) multilayers on glass microscope cover slips were doped with small levels of a fluorescently labeled silane coupling agent (FLSCA). The FLSCA/GPS layers were characterized by SEM, contact angle, and fluorescence spectroscopy. An earlier report indicated that the emission of grafted FLSCA was sensitive to the surface energy of the silane layer [16], and the resin dynamics in the buried interfacial region [17]. In this work we have demonstrated that grafted FLSCA is sensitive to additional factors that can

influence polymer/substrate adhesion. The dye is sensitive to the structure of the silane coupling agent layer, suggesting that thinner silane layers are more tightly bound with the glass surface. In addition, FLSCA is sensitive to the interaction between the silane layer and the curing resin. Smaller fluorescence shifts during resin cure from thick coupling agent layers suggest that the resin molecules do not penetrate completely or react completely with the thicker layers. The novel technique, presented in this paper, to probe the buried interfacial structure in situ has the potential for its application to the study of interfacial chemical reactions.

References

- [1] T. Nguyen, C. Han, R.R. Cavanagh, R. Ryntz, Report from 2nd Workshop on Characterization and Modeling of the Interface/Interphase of Polymeric Materials and Systems, NISTIR 6352, 1998.
- [2] A.J. Kinloch, Adhesion and Adhesives: Science and Technology, Chapman and Hall, New York, 1987.
- [3] R.P. Wool, Polymer Interfaces: Structure and Strength, Hasner/Gardner, New York, 1995.
- [4] E.P. Plueddemann, J. Adhesion 2 (1970) 184.
- [5] L.T. Drzal, in: K. Dusek (Ed.), Advances in Polymer Science, Springer-Verlag, Berlin, 1986, p. 1.
- [6] W.-L. Wu, W.J. Orts, C.J. Majkrzak, D.L. Hunston, Polym. Eng. Sci. 35 (1995) 1000.
- [7] N. Nishiyama, R. Schick, H. Ishida, J. Colloid Interface Sci. 143 (1991) 146.
- [8] M.W. Daniels, J. Sefcik, L.F. Francis, A.V. McCormik, J. Colloid Interface Sci. 219 (1999) 351.
- [9] E.T. Vandenberg, L. Bertilsson, B. Liedberg, K. Uvdal, R. Erlandsson, H. Elwing, I. Lundstrom, J. Colloid Interface Sci. 147 (1991) 103.
- [10] S.R. Culler, H. Ishida, J.L. Koenig, J. Colloid Interface Sci. 106 (1985) 334.
- [11] H. Ishida, J.D. Miller, Macromolecules 17 (1984) 1659.
- [12] N. Nishiyama, R. Schick, K. Horie, H. Ishida, Polym. Commun. 31 (1990) 380.
- [13] T.W.H. Wang, F.D. Blum, L.R. Dharani, J. Mater. Sci. 34 (1999) 4873.
- [14] L. Gong, A.D. Friend, R.P. Wool, Macromolecules 31 (1998) 3706.
- [15] L. Isoon, R.P. Wool, Macromolecules 33 (2000) 2680.
- [16] J.L. Lenhart, J.H. van Zanten, J.P. Dunkers, C.G. Zimba, C.A. James, S.K. Pollack, R.S. Parnas, J. Colloid Interface Sci. 221 (2000) 75.
- [17] J.L. Lenhart, J.H. van Zanten, J.P. Dunkers, R.S. Parnas, Macromolecules 34 (2001) 2225.
- [18] E.P. Plueddemann, Composite Materials: Interfaces in Polymer Matrix Composites, Vol. 6, Academic Press, New York, 1974.
- [19] NIST does not endorse any products. Identification of a commercial product is made only to facilitate experimental reproducibility and to adequately describe experimental procedure.
- [20] D.R. Robello, J. Polym. Sci. Part A: Polym. Chem. 28 (1990) 1.
- [21] F. Chaput, D. Riehl, Y. Lévy, J.-P. Boilot, Chem. Mater. 5 (1993) 589.
- [22] F. Chaput, D. Riehl, J.-P. Boilot, K. Cargnelli, Canva, Y. Lévy, A. Brun, Chem. Mater. 8 (1996) 312.
- [23] J.L. Lenhart, J.H. van Zanten, J.P. Dunkers, R.S. Parnas, Langmuir 16 (2000) 8145.
- [24] C.J. Brinker, G.W. Scherer, Sol Gel Science: The Physics and Chemistry of Sol Gel Processing, Academic Press, Boston, 1990.
- [25] M.E. Schrader, J. Adhesion 2 (1970) 202.
- [26] J.R. Lakowicz, Principles of Fluorescence Spectroscopy, Plenum Press, New York, 1983.
- [27] J. Gonzalez-Benito, J.C. Cabanelas, A.J. Aznar, M.R. Vigil, J. Bravo, J. Baselga, J. Appl. Polym. Sci. 62 (1996) 375.
- [28] H.J. Kang, F.D. Blum, J. Phys. Chem. 95 (1991) 9391.

- [29] N. Nishiyama, K. Horie, T. Asakura, *J. Colloid Interface Sci.* 129 (1989) 113.
- [30] S.G. Croll, *J. Appl. Polym. Sci.* 23 (1979) 847.
- [31] K.F. Lin, F.W. Wang, *Polymer* 35 (1994) 687.
- [32] R. Lapouyade, A. Kuhn, J.-F. Letard, W. Rettig, *Chem. Phys. Lett.* 208 (1993) 48.
- [33] H. Gruen, H. Gerner, *J. Phys. Chem.* 93 (1989) 7144.
- [34] D.L. Woerdeman, J.K. Sporre, K.M. Flynn, R.S. Parnas, *Polym. Compos.* 18 (1997) 518.
- [35] C.S.P. Sung, J.C. Song, *Macromolecules* 26 (1993) 4148.
- [36] O. Pekcan, Y. Yilmaz, O. Okay, *Polymer* 38 (1997) 1693.
- [37] T. Kobayashi, S. Takahashi, F. Nobuyuki, *J. Appl. Polym. Sci.* 49 (1993) 417.
- [38] A. van Blaaderen, A. Vrij, *Langmuir* 8 (1992) 2921.